J Appl Electrochem (2011) 41:1065–1075
DOI 10.1007/s10800-011-0288-x

ORIGINAL PAPER

Voltage-step transient on circular electrodes

Ondrej Wein · Valentin V. Tovchigrechko

Received: 5 December 2010 / Accepted: 10 March 2011 / Published online: 26 March 2011

Abstract Using the well-known Cottrell asymptote, voltage-step transient (VST) experiments in a two-electrode cell may provide data on the bulk concentration and diffusion coefficient of a working depolarizer, essential for interpretation of liming-diffusion-current (LDC) experiments. However, the Cottrell asymptote is never applicable in the early stages of the voltage-step transient process. There are three additional transport resistances to the basic diffusion transport that cannot be neglected at extremely high initial currents: Faradaic resistance at the working electrode surface, overall Ohmic losses in the electrochemical cell, and a possible galvanometric constraint in the outer circuit, involving the galvanometer, current follower, potentiostat, etc. The effect of these additional transport resistances on the transient current at higher polarization voltage is non-linear. In the present analysis, a 1D approximation is used, assuming tacitly uniform accessibility of the working electrode and negligible transport resistances at the counter electrode. The Faradaic resistance of a redox couple $O + ne^- = R$ according to Butler–Volmer electrode kinetics is considered. The results of 1D theory are corrected for edge effects using the Oldham asymptote. The effect of convection at longer times is included using the recent model of a transient process for circular working electrodes in the LDC regime.

Keywords Voltage-step transient · Cottrell asymptote · Ohmic loss · Faradaic resistance · Galvanometric constraint · Butler–Volmer kinetics

O. Wein (✉) · V. V. Tovchigrechko
Institute of Chemical Process Fundamentals of ASCR, v.v.i., Rozvojova 135, 16502 Prague 6-Suchdol, Czech Republic
e-mail: wein@icpf.cas.cz
URL: http://home.icpf.cas.cz/wein

List of symbols

Variables

A	Effective area of working electrode, m^2
A_∞	area of ideally smooth working electrode, m^2
B	$\equiv D_O^{1/2} c_O^B / D_R^{1/2} c_R^B$, transport parameter
C	Cottrell coefficient (m $s^{-1/2}$)
c, $c_{O,R}^{B,W}$	Molar concentration of depolarizers and their boundary values (mol m^{-2} s^{-1})
D, $D_{O,R}$	Coefficient of diffusion; values for the components (m^2 s^{-1})
$d_T^{-1/2}$	Semi-integral operator
E	= Exp[P]
f	= $(E - 1)/(E+B)$, Nernst–Petersen factor
G	= k_G/k_S, normalized galvanometric constraint
I	Current (A)
$J_{O,R}$	Diffusion fluxes of depolarizers at surface (mol m^{-2} s^{-1})
K	= $k_{BV}(c_O^B)^{1-\beta}(c_R^B)^{\beta}$, modified rate constant (mol m^{-2} s^{-1})
k	= $I/(nFA\ c_{work}^B)$, mass-transfer coefficient (m s^{-1})
k_{BV}	Rate constant factor in Butler–Volmer kinetics (m s^{-1})
k_C	= $U/(nFAR_C c_{work}^B)$, Ohmic limit for $k(t)$ (m s^{-1})
k_G	= $I_G/(nFA\ c_{work}^B)$, galvanometric constraint (m s^{-1})
k_S	= μk_C, starting (upper) limit for $k(t)$ (m s^{-1})
L_C	Equivalent resistor length (m)
M	$\equiv K/k_C$
nF	The charge transfer per 1 mol of the working depolarizer (C mol^{-1})
$N = N(T)$	$\equiv k/k_S$, normalized flux

N_L	Solution to the linearized transport equation
O, R	Oxy- and Red- forms of the redox couple, $O + ne^- \leftrightarrow R$
P	$\equiv -UnF/RT$, normalized voltage; $F = 95608$ C mol^{-1}, Faraday constant; $R = 8.313$ J K^{-1} mol^{-1}, universal gas constant; T, absolute temperature
R_C	Ohmic resistance of the cell (Ω)
t	Time from the initial voltage step
t_S	$\equiv (C/k_S)^2$, characteristic lag time (s)
T	$\equiv t/t_S$, normalized time
U	Constant voltage between working and counter electrodes (V)
$W = W(T)$	$\equiv 1 - c_O^W/c_O^B$, normalized concentration driving force (for cathodic depolarizer)
z	Normal distance to the working electrode (m)
β	Symmetry coefficient in Butler–Volmer kinetics
$\Lambda[N]$	United boundary-value constraint for the concentration driving force
∂_T	Partial derivative with respect to T
μ	$\equiv k_S/k_C$
θ	$= \pi/4$, the asymptotic divide time
η	$= U - IR_C$, overvoltage (V)
κ	Specific conductivity of the bulk solution (S m^{-1})
δ	$\equiv D/\lvert k\rvert$, Nernst diffusion layer thickness (m)

Indices (superscripts and subscripts)

$c^{B,W}$	*B*ulk or *W*all compositions of the solution
C	Ohmic resistance of the two-electrode cell
G	Galvanometric constraint
NP	Reversible electrodes according to the Nernst–Petersen rule
$c_{O,R}$	*O*xy- or *R*ed- form of redox couple
S	Start of the process

Abbreviations

ED	Electrodiffusion
LDC	Limiting diffusion current
VST	Voltage-step transient

1 Introduction

The voltage-step transient (VST) process in an electrochemical cell with a motionless electrolyte solution can be of interest both for studying the kinetics of electrode reactions [1–3] and for measuring the diffusion coefficients of depolarizers [4, 5]. The VST process in the three-electrode electrochemical cells (with reference electrode) is commonly taken as a potentiodynamic one, i.e. with negligible additional transport resistances in the electrochemical cell and outer circuits. Such an assumption cannot be strictly right [1–5], for at least two reasons:

- It tacitly assumes infinite current—i.e. zero transport resistances—at the start according to well-known Cottrell asymptote, $I \sim t^{-1/2}$. Consequently, other transport mechanisms must play a dominating role in the early stage of the VST process even in a three-electrode cell configuration driven by a potentiostat with feedback from a reference electrode [1].
- The potentiodynamic control is based on the assumption that the feedback reading of the reference electrode is accurate and instantaneous. This need not be right, as the Luggin capillary of the reference cannot be placed close enough to the working electrode surface and its response to fast changing electrochemical potential is not quick enough [1].

A reasonable approach to studying the early stages of the VST process would be to work with two-electrode cells (no reference electrode) and to include corresponding additional transport resistances into the theory of the process [6–8]. There are several transport mechanisms that can control the transient current at a given voltage, even with neglected transport resistances at the counter electrode and in bulk solution of a two-electrode cell:

- Cottrellian transient diffusion, which includes equilibrium at the working electrode
- Ohmic losses in the close neighbourhood of the working electrode
- Faradaic losses on the working electrode due to electrode kinetic limitations
- Galvanometric constraints due to limitations in the outer circuit

In the present work, all these simultaneous transport resistances are accounted for in a 1D approximation, with an arbitrary constant voltage U between the working and counter electrode.

2 Problem statement

2.1 Transport equations

Concentrations $c_{O,R}^B$ of both depolarizers in the bulk, i.e. at a large distance ($z \to \infty$) from the transport-active surface, also provide the initial conditions, $c_{O,R}(t = 0) = c_{O,R}^B$. For the couple of redox depolarizers O, R involved in the charge-transfer electrode reaction, $O + ne^- \leftrightarrow R$, the diffusion fluxes $J_{O,R}$ are linked through the stoichiometry, $J_O = -J_R$. The transport equations can be given in a

differential form (2nd Fick law), $\partial_t c_{O,R} = D_{O,R}\partial_{zz} c_{O,R}$. The current density and mass-transfer coefficients are then taken from the surface concentration gradients,

$$I/(nFA) = J_O = -J_R, \tag{1}$$

$$J_{O,R} = -D_{O,R}\partial_z c_{O,R}|_{z=0}, \tag{2}$$

$$k_{O,R} = J_{O,R}/c^B_{O,R}. \tag{3}$$

The same boundary-value problem can be formulated using semiintegral operators [9],

$$d_t^{-1/2}F(t) \equiv \pi^{-1/2}\int_s^t (t-s)^{-1/2}F(s)\mathrm{d}s,$$

which interrelate the mass-transfer coefficients with the normalized wall concentrations $w_{O,R}(t)$,

$$d_T^{-1/2}k_{O,R}(t) = D_{O,R}^{1/2}w_{O,R}(t), \tag{4}$$

$$w_{O,R}(t) = 1 - c^W_{O,R}(t)/c^B_{O,R}. \tag{5}$$

Note the obvious stoichiometry constrains according to Eqs. 1–3:

$$Bw_O(t) + w_R(t) = 0, \tag{6a}$$

$$Bk_O(t) + k_R(t) = 0, \tag{6b}$$

$$B \equiv D_O^{1/2}c_O^B D_R^{1/2}c_R^B, \tag{7}$$

which offer an option to formulate and solve the problem for either the O or R form of the redox couple. To avoid ambiguities, the O, R subscripts are abandoned to prefer simpler symbols $k(t)$, $w(t)$, D, $c^{B,W}$, etc., related to the working depolarizer, i.e. for O in the cathodic regime ($U < 0$, $P > 0$) and R in the anodic regime ($U > 0$, $P < 0$).

Until the start at $t = 0$, the electrochemical system is kept in equilibrium, $k = 0$, $w = 0$. To a given problem with the unknown fields $k(t)$, $w(t)$ and a given course of the electrode overvoltage, $\eta = \eta(t)$, the closing constraint follows from the kinetic equation of charge transfer at the working electrode surface. For Butler–Volmer kinetics this constraint is:

$$k/K = (1-w)E^{\beta\eta/U} - (1+Bw)E^{-(1-\beta)\eta/U}, \tag{8}$$

where

$$K = k_{BV}\left(c_O^B\right)^{1-\beta}\left(c_R^B\right)^{\beta},\ P = -UnF/RT,\ E = \mathrm{Exp}[P].$$

If both electrodes are made from the same material, then $\eta = U = 0$ corresponds to the equilibrium state. With negligibly small Ohmic resistance it still holds that $\eta = U$. To include the effect of Ohmic losses, let us express R_C via an effective resistance length L_C between the electrodes and conductivity κ of the bulk solution, $R_C = L_C/\kappa$:

$$\eta(t)/U = 1 - IR_C/U = 1 - k(t)/k_C, \tag{9}$$

$$k_C = -\kappa U/\left(nFAc^B L_C\right) \tag{10}$$

At constant overvoltage η, the VST problem simplifies to a potentiodynamic one. If, in addition, the Faradaic resistance is negligible, $K \to \infty$, the process is controlled only by the transient diffusion of the depolarizers under Nernst–Petersen equilibrium surface conditions. The corresponding simplified linear theory provides the well-known Cottrell solution [2]. A simplified linear theory of VST is also available including the Faradaic resistance (finite K), if the P is small enough to use the linearized [2, 7] approximation $E^{\alpha} = 1 + \alpha P$.

In the present work, VST is analyzed by considering all the four kinds of transport resistance at a finite voltage. In such a case, the Ohmic loss according to Eq. 9 (second part of the equation) introduces a substantial non-linearity, which has been analyzed for negligible Faradaic losses in [5]. Our results for the combined Ohmic and Faradaic resistances, published in Russian [7], provide only qualitative estimates of limited relevance. The effect of additional resistance in the outer circuit (galvanometric constraint) is analyzed here for the first time.

2.2 Cottrell asymptote

With negligible Ohmic and Faradaic losses, $k/k_C \to 0_+$, $k/K \to 0_+$, the VST process is driven only by the concentration overpotential $\eta = U$, with diffusion resistance according to Eq. 4 under local equilibrium at the working electrode (the Nernst–Petersen equation):

$$w = (E-1)/(E+B), \tag{11}$$

which clearly follows from Eq. 8.

Solution of this simplified problem according to Eq. 4 with constant w, known as the *Cottrell problem*, see [3], can be written as

$$k(t) = C(\pi t)^{-1/2}, \tag{12}$$

where $C = fD^{1/2}$, $f = (E-1)/(E+B)$.

In the cases $|P| \to \infty$, the cathodic ($P = +\infty$, $E = \infty$) or anodic ($P = -\infty$, $E = 0$) limiting-diffusion-current (LDC) regime is achieved. These asymptotes are fully controlled by transient diffusion of the corresponding working depolarizer. For the cathodic reduction: $f = 1$, $w_O = 1$, $w_R = -B$. For the anodic oxidation: $f = -1/B$, $w_R = 1$, $w_O = -1/B$.

2.3 Start of the transient process

Immediately after switching on the cell, the diffusion resistance is negligible compared with the other transport

resistances, i.e. $w \to 0$. The starting value $k(t=0) = k_S$ may be found solving the Eq. 8 for μ with given M:

$$0 = E^{\beta(1-\mu)} - E^{-(1-\beta)(1-\mu)} - \mu M, \tag{13}$$

where $\mu \equiv k_S/k_C$, $M \equiv k_C/K$. For negligible Faradaic resistance: $M = 0$, $\mu = 1$. For negligible Ohmic losses: $M = \infty$, $\mu M = k_S/K = E^{\beta} - E^{\beta-1}$. For small enough overvoltage: $\mu = 1 - M/(M + P)$. In all other cases: $0 < \mu < 1$.

Even if the voltage is measured or controlled by an outer circuit without affecting the current (by some serially built in resistances) the outer circuit can be equipped by a current threshold I_G that cannot be overcome. In such a case, the early stage of a VST proceeds galvanostatically, $k = k_G = I_G/(nFAc^B)$. In contrast to common potentiodynamic methods with a three-electrode cell [3], the corresponding changes of the electrochemical potential cannot be monitored in a two-electrode cell (no reference electrode), but they strongly affect the currents below the threshold in the later stages of a VST process.

2.4 Normalization of the problem

The normalized flux N and normalized time T are introduced in such a way that

(i) the starting value of N (diffusion resistance negligible) is normalized to $N = 1$ at $T = 0$,
(ii) the long-time asymptote is in the common Cottrell form, $N \to (\pi T)^{-1/2}$ for $T \to \infty$.

This specification is fulfilled by the settings:

$$N = k/k_S, \quad T = t/t_S, \quad t_S = (C/k_S)^2, \quad W = w \tag{14}$$

The problem can be now formulated as a single non-linear semiintegral equation for the function $N = N(T)$, $0 \le N \le 1$, $0 \le T < \infty$:

$$d_T^{-1/2} N(T) = W(T) = \Lambda[N(T)], \tag{15}$$

$$\Lambda[N] = \frac{E^{\beta(1-N\mu)} - E^{-(1-\beta)(1-N\mu)} - N\mu M}{f\left(E^{\beta(1-N\mu)} + BE^{-(1-\beta)(1-N\mu)}\right)}. \tag{16}$$

Details of analytic approximations and numerical solving are available in the research report O. Wein: *Voltage-step transient in redox systems II. 1D approximation,* Res. Rep. ICPF 2010/6, in http://home.icpf.cas.cz/wein.

2.5 Useful symmetries

There are four independent parameters $\{\beta, B, P, M\}$ or $\{\beta, B, P, \mu\}$ to the problem. The transformation $\{\beta \to 1 - \beta, B \to B^{-1}, P \to -P, M \to M, \mu \to \mu\}$, which physically corresponds to changes from cathodic to anodic polarization, guarantees that any actual case can be studied with a positive P. In particular, for the special symmetry case $\{B = 1, \beta = (1 - \beta) = 1/2\}$, the problem is invariant with respect to polarity change, $P \to -P$.

3 Solving the transient problem

3.1 Special cases

At negligible both Ohmic and Faradaic losses, $W = 1$, the solution to the transport equation (15) is approximated by the Cottrell asymptote, $N(T) = (\pi T)^{-1/2}$.

At very small overvoltage, $P \to 0$, $f \approx P/(1 + B)$, the initial condition (13) simplifies to $\mu/M \approx P(1 - \mu)$ and the constraint (16) can be linearized to $\Lambda[N] \approx 1 - N$. There is a simple analytic solution to (15) for this special case [1, 3, 8]:

$$N(T) = N_L[T] \equiv \mathrm{Exp}[T]\mathrm{Erfc}\left[T^{1/2}\right]. \tag{17}$$

With negligible Faradaic resistance, i.e. $M = 0$, $\mu = 1$, the constraint (16) reduces to

$$\Lambda[N] = \frac{E^{1-N} - 1}{f(E^{1-N} + B)}. \tag{18}$$

The related mathematical problem (15) for this case may be solved using asymptotic approximations or numerical methods.

3.2 Short-time asymptote

At short enough time after the start, $T \to 0$, the flux is close enough to its starting value, $N \to 1$. The related non-linear driving force according to Eq. 15 can be approximated as

$$W = \Lambda[N] \approx \psi(1 - N), \tag{19}$$

$$\psi = \frac{E^{(1-\mu)}(1 + \beta\mu P) - (1 + (\beta - 1)\mu P)}{f(E^{(1-\mu)} + B)}. \tag{20}$$

The corresponding approximation to the transport equation (15):

$$N(T) = N_L[\psi^{-2} T] \tag{21}$$

3.3 Long-time asymptote

At long enough time, $T \to \infty$, the flux follows the Cottrell asymptote, $N \approx (\pi T)^{-1/2}$. When looking for a higher-order expansion, both the long-time and short-time asymptotes should be matched at the dividing time between short-time and long-time regime, $\theta = \pi/4$,

$$N(T) \approx (\pi T)^{-1/2}\left(1 + b_1 T^{-1} + \cdots\right), \tag{22}$$

$$b_1 = \frac{\theta\pi(8(1-\pi\psi) - 9(Y-\psi^2) + 6\psi^2 N_L(\theta)}{24(2-Y)} - \frac{\psi^3 - \psi^4 N_L(\theta)}{2(2-Y)}, \quad (23)$$

$$Y = \frac{E^{1-\beta\mu} - E^{(1-\beta)\mu}}{E-1} + \frac{\mu PE}{f(E+B)}. \quad (24)$$

3.4 Galvanometric constraint

With a finite threshold $I \le I_G$ in the outer circuit, the initial current cannot overcome this limit. As a result, the current in an early stage, $T < \theta$, is constant, $N(T) = G$, $G \equiv k_G/k_S$, and the driving force $W(T)$ is governed by the galvanostatic regime according to Eq. 15,

$$W(T) = d_T^{-1/2} G = \frac{2}{\pi} G(\pi T)^{1/2}. \quad (25)$$

This regime lasts until a time T_G, when $W(T)$ increases to the threshold value $W_G = W(T_G)$ according to the constraints following from Eq. 15:

$$W_G = \frac{2}{\pi} G(\pi T_G)^{1/2} = \Lambda[G]. \quad (26)$$

After passing the singular point $T = T_G$, the VST process continues in a normal way, according to Eq. 15. If the both Faradaic resistance and Ohmic loss are negligible at given galvanometric constraint, i.e. at $G = 1$, there is a simple solution to the problem with $T_G = \theta$:

$$N(T) = \begin{cases} 1, & T < \theta \\ \frac{2}{\pi}\mathrm{Arccot}\left(\sqrt{T/\theta - 1}\right), & T > \theta \end{cases}. \quad (27)$$

Obviously, this solution provides a short-time extension to the long-time Cottrell asymptote.

If the Faradaic resistance and Ohmic loss are accounted for, $G < 1$, the problem may be solved numerically. Asymptotic analysis for this case is analogous to that in Sect. 3.3 but slightly simpler, as the short-time increment for $T < T_G$ is known, $N(T_G) = G$. The trial form according to Eq. 22 results in:

$$b_1 = T_G\left(18Y + 15GT_G - 32\sqrt{T_G/\pi}\right)/(12(Y - 4T_G)). \quad (28)$$

3.5 Numerical analysis

The applied numerical scheme is based on a discrete representation of the function $N(T)$ with a constant-step grid but differs from the older one [7] in several respects:

- Instead of its inverse form [6], the transport equation is solved in its direct form, $d_T^{-1/2} N(T) = \Lambda[N(T)]$
- Instead of a relaxation procedure [6], the resulting non-linear problem for the local $N(T)$ is solved using the direct Newton iteration.

The semiintegral of a function $N(T)$ can be transformed, using the linear transformation $T = m\Delta T$, $s = i\Delta T$, to the form

$$d_T^{-1/2} N(T) \equiv \pi^{-1/2} \int_0^T \frac{N(s)\mathrm{d}s}{(T-s)^{1/2}} = (\Delta T/\pi)^{1/2} \int_0^m \frac{N(i\Delta T)\mathrm{d}i}{(m-i)^{1/2}}. \quad (29)$$

If the function $N(T)$ is specified only in the discrete points of a homogeneous grid, $N_i = N(T_i)$, $T_i = i\Delta T$, $i = [0\ldots m]$, its semiintegral can be approximated by a suitable discrete linear formula:

$$d_T^{-1/2} N(T) \approx (\Delta T/\pi)^{1/2} \sum_{i=0..m} S_{m,i} N_i. \quad (30)$$

Starting with a known discrete representation $N(T_i) = N_i$ for $i < m$, the discrete form of the transport equation for unknown $N(T_m) = N_m$ can be written as

$$(\Delta T/\pi)^{1/2} \left(\sum_{i=0\ldots m-1} S_{m,i} N_i + S_{m,m} N_m \right) = \Lambda[N_m]. \quad (31)$$

This non-linear equation for N_m can be solved e.g. by *regula falsi* method using value N_{m-1} as a starting estimate. The coefficients $S_{m,i}$ in Eq. 31 can be constructed following various approximation schemes. Oldham and Spannier [9] suggested the formula R2, based on a ramp local approximation of $N(T)$, as used also in [6, 7]:

$$S_{m,i} = \frac{4}{3}(m-1-i)^{3/2} + \frac{8}{3}(m-i)^{3/2} - \frac{4}{3}(m+1-i)^{3/2}, \quad (32a)$$

$$S_{m,0} = \frac{8}{3}(m-1)^{3/2} - \frac{4}{3}(2m-3)m^{1/2} \quad (32b)$$

3.6 Selected results of numerical analysis

Results of the numerical analysis provide the normalized transient currents (current densities, mass-transfer coefficients) $N = N(T)$ for a given set $\{\beta, B, P, M, G\}$ of the normalized process parameters. In particular, β gives the symmetry exponent in the Butler–Volmer model; B, concentration ratio of the both depolarizers; P, the normalized voltage; M, the ratio of maximum possible currents when either Ohmic or Faradaic resistance is negligible; and G, an additional galvanometric constraint. In the cases with no galvanometric constraint, the parameter $G = 1$ is omitted.

Three basic asymptotes are shown in Fig. 1: the linear asymptote $N(T) = N_L[T]$ according to Eq. 17, the classic Cottrell asymptote $N(T) = (\pi T)^{-1/2}$, and the extended Cottrell asymptote under a galvanometric constraint according to Eq. 27. Note that the case $M = 0$ corresponds

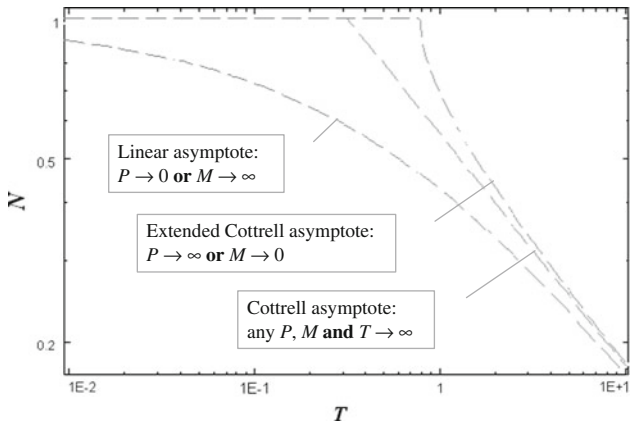

Fig. 1 Global asymptotes in the $\{M, P\}$ space

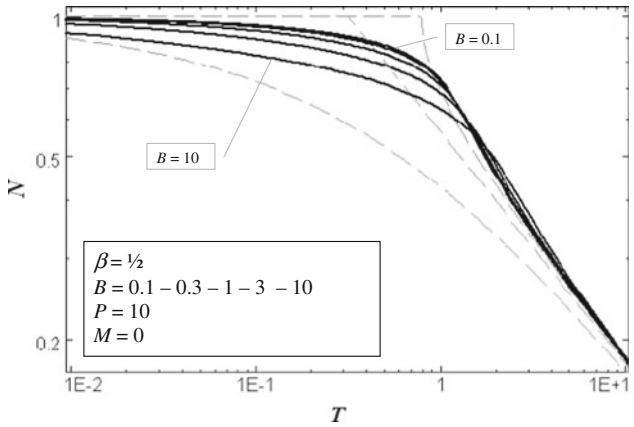

Fig. 3 Normalized transient currents for negligible Ohmic loss, effect of composition

to negligible Faradaic resistance while $M \to \infty$ corresponds to negligible Ohmic loss, i.e. to potentiodynamic control of the VST process. The numerical results are shown in the plots, identified by the operation set $\{\beta, B, P, M, G\}$, and supplied with the basic asymptotes (gray curves in the background).

The trends under varying P are shown in Fig. 2. At low P, say $P < 1$, the linear asymptote provides a reasonable approximation to $N(T)$ for any finite values of $\{P, M\}$. At extremely high P, say $P > 50$, the numerical results are approximated fairly well by the extended Cottrell asymptote, which corresponds to the LDC regime.

The trends under varying B are shown in Fig. 3. As the diffusion coefficients of both depolarizes in a redox couple are commonly close to each other, the change of B corresponds mainly to the concentration ratio. At extremely high or low P, the $N(T)$ curves depend on B only slightly.

The trends under varying M are shown in Fig. 4a and b for medium and high P. The $N(T)$ curves at very low P approach the linear asymptote for any M. At finite P, there is an additional condition $M \gg \mathrm{Exp}[\beta P]$ for approaching the linear asymptote, compare the Fig. 4a with b.

The effect of galvanometric constraint is shown in Fig. 5. Note that in the cases $G \geq 1$, there is no such constraint, as the all actual currents are below the threshold value.

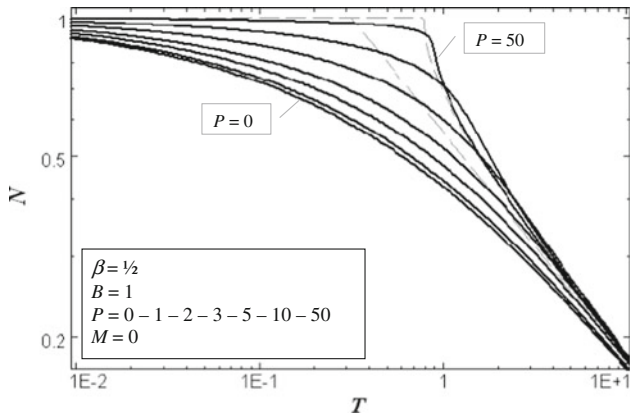

Fig. 2 Normalized transient currents for negligible Ohmic loss, effect of overvoltage

4 Semiempirical extension of the VST theory for longer times

The theory presented up to now neglects the convection and 3D diffusion, as these effects play no role at very short times, say $t < 0.1$ ms. In this section, the known approximate models of the transient edge effects and convective diffusion are used to a semi-empirical extension of the presented theory. Note that a real, experimentally available transient mass-transfer coefficient $k(t)$ is related to the normalized transient curve $N(T)$ through the normalizing parameters $\{k_S, t_S\}$, deduced from the start conditions and Cottrell asymptote:

$$k(t) = k_{NT}(t) \equiv k_S N(t/t_S) \tag{33}$$

4.1 Oldham asymptote: Edge effect in motionless liquid

Oldham [10] suggested an asymptotic extension to the classic Cottrell 1D result by considering edge effects close to the perimeter of a finite working electrode, assuming LDC regime (i.e. $w = 1$). Aoki and Osteryoung [11] solved the VST problem for a reversible electrode. Actually, they have shown that the approach by Oldham [10] can be extended from LDC regime to the case of reversible electrodes, i.e. for the surface constraint in the form $w = f$. Following such an approach for circular (disk)

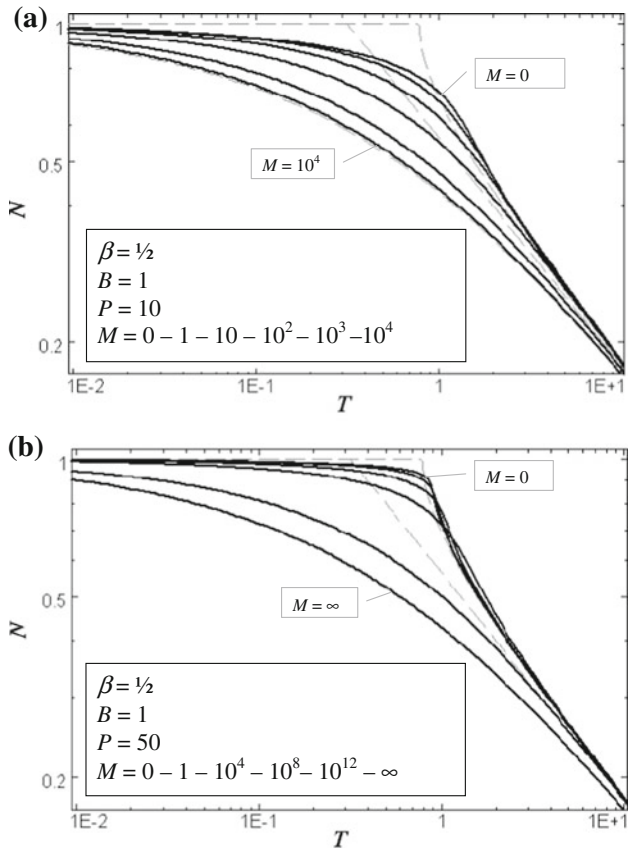

Fig. 4 Normalized transient currents, effect of Ohmic and Faradaic resistance: **a** medium overvoltage ($P = 10$, $U \approx 200$ mV); **b** high overvoltage ($P = 50$, $U \approx 1000$ mV)

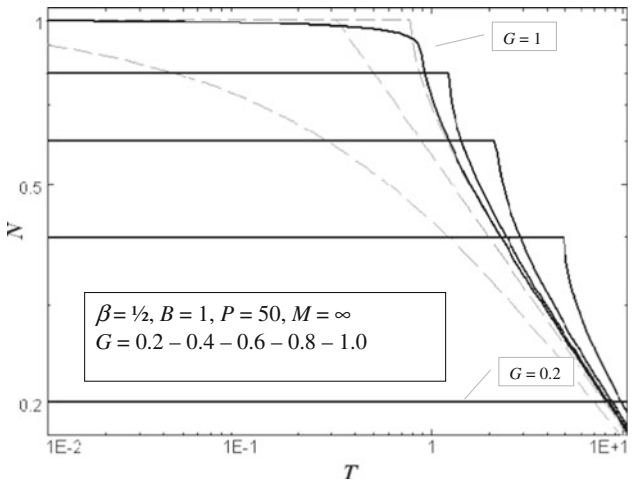

Fig. 5 Normalized transient currents for negligible Ohmic and Faradaic loss, effect of galvanometric constraint

working electrodes, the original Oldham formula can be extended to:

$$k(t) = \frac{\pi}{4}k_\infty + C_{NP}(\pi T)^{-1/2}, \tag{34}$$

$$C_{NP} = fD^{1/2}. \tag{35}$$

For steady diffusion to a reversible disk micro-electrode of radius R in the motionless liquid:

$$k_\infty = fD/R. \tag{36}$$

4.2 An ultimate asymptote

Under LDC regime, i.e. neglecting all but diffusion resistances, the overall transient course of fluxes was analyzed in [5]. In the present notation, and extending the LDC regime results to reversible electrodes, the final result can be written as:

$$k(t) = \begin{cases} \frac{\pi}{4}k_\infty + C_{NP}(\pi t)^{-1/2}\left(1 + \frac{1}{2}(t/t_0)^{3/2}\right), & t < t_0 \\ k_\infty, & t > t_0 \end{cases}, \tag{37}$$

where

$$t_0 = (C_{NP}/k_\infty)^2\left(\frac{2}{3}\pi^{1/2}\left(1 - \frac{\pi}{4}\right)\right)^2 = \left(R^2/D\right)\left(\frac{2}{3}\pi^{1/2}\left(1 - \frac{\pi}{4}\right)\right)^2. \tag{38}$$

The steady-state (ultimate) mass-transfer coefficient k_∞ for a disk electrode in a steady flow with the wall shear rate γ, given in [5], can be also modified to an estimate for reversible electrodes:

$$k_\infty = f(1 + \beta_\infty)k_L, \tag{39}$$

where $k_L = 0.6866D^{2/3}(\gamma/R)^{1/3}$ stands for k under LDC regime in the diffusion-layer (Leveque) approximation and $\beta_\infty = 1.0131H^{-1} - 0.2753H^{-4/3} + 0.0065H^{-2}$ for the correction on 3D edge effects at sufficiently high Peclet number, $H = 0.5425R(\gamma/D)^{1/2}$.

4.3 Effect of surface roughness

The theory presented up to now assumes an ideally smooth electrode surface of a constant area $A = A_\infty$, $k = k_{\text{smooth}}$. One of the available microscopic theories of the surface roughness [12] assumes that the transport of components proceeds across the diffusion layer of varying thickness δ, which adheres to a rough surface. If δ is small enough in comparison with the length scale of the roughness, the effect of the surface roughness can be based on the concept of enhanced area $A = A(\delta) \geq A_\infty$. The correction then consists in applying the enhanced area $A(\delta)$ instead of its smooth asymptote A_∞, $k/k_{\text{smooth}} = A_\infty/A(\delta) < 1$, even for an arbitrarily large δ. The present application of the surface-roughness model in describing the VST process consists in identifying the δ with the instantaneous Nernst diffusion thickness [5],

$$\delta(t) = D/k_{\text{smooth}}(t). \tag{40}$$

In particular, the diffusion thickness under LDC regime is $\delta(t) = (\pi Dt)^{1/2}$ within the Cottrell asymptote and $\delta(\infty) = 1.456(DR/\gamma)^{1/3}$ within the Leveque asymptote.

The bimodal (four-parameter) version of the surface roughness model assumes a pyramidal surface [12],

$$A/A_\infty = E_A(\delta) \equiv \chi(E_1, \delta/\lambda_1)\chi(E_2, \delta/\lambda_2), \tag{41}$$

where $\{\lambda_1, \lambda_2\}$ stand for mutually perpendicular characteristic wave lengths, and $\{E_1, E_2\}$ stand for the ultimate area enhancement at $\delta = 0$, and

$$\chi(E, \varepsilon) = \begin{cases} \varepsilon^{-1}\,\text{ArcSin}(\varepsilon), & \varepsilon < \sqrt{1 - E^{-2}} \\ \sqrt{E^2 - 1} + \text{ArcSin}(E^{-1}) - \frac{\pi}{2}, & \varepsilon > \sqrt{1 - E^{-2}} \end{cases}. \tag{42}$$

5 Experimental

The main purpose of the VST experiments was to test the complete transport model for the electrochemical systems with very fast electrode reaction. Thus, two different series of VST experiments were carried out:

- Short-time VST experiments of duration about 10 ms with sampling density 100 kHz taken in a simple beaker cell with a motionless liquid. The data cover the early period of VST, when the current is independent of convection and 3D diffusion.
- Long-time VST experiments of duration about 1000 ms with sampling density 1 kHz taken in the electrodiffusion (ED) calibrator. At high enough wall shear rate γ, the $k - t$ data also cover the steady state limit k_∞.

Both the short-time and long-time VST experiments for a given ED probe and a given electrolyte solution were conducted on several levels of polarization voltage U ranging from +800 mV (anodic LDC regime) to −1200 mV (cathodic LDC regime).

To test the extent of edge effects, three Pt well-calibrated *portable ED probes* with circular working electrodes of different radii were used. The design of all the portable ED probes was the same. A working electrode from Pt wire, electrophoretically covered with an insulating layer and connected to a long Cu wire, was glued by epoxy resin into a stainless steel tube of outer diameter 5 mm. The front surface of the stainless tube may eventually serve as a counter electrode. The probe was equipped with a universal three-cable connector. Front photographs of the working electrodes are shown in Fig. 6. Their calibration characteristics are listed in Table 1 and plotted in Fig. 7.

The *ED cell* for the short-time VST measurements consisted of a 100 ml laboratory beaker immersed in a thermostatic bath. It was equipped with a deck for fixing of the working electrodes and introducing inert gas, and with a large cylindrical Pt counter electrode of area 2000 mm^2. The liquid in the beaker could be agitated with a magnetic stirrer, sealed in a plastic cover.

A scheme of the *ED calibrator*, used for the long-time VST measurements, is shown in Fig. 8. Its viscometric configuration consists of a fixed upper deck 1 and a rotating dish 2. The horizontal gap between deck and dish of thickness h was filled with electrolyte solution. For the ED probe 3 located at distance r from the axis, the wall shear rate can be calculated as

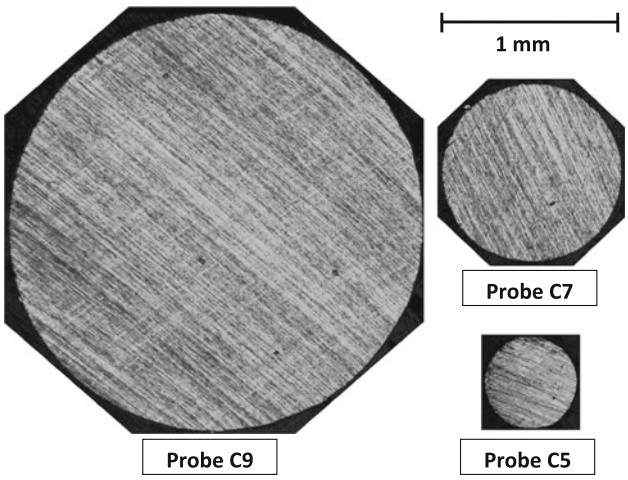

Fig. 6 Front photographs of the used working electrodes

Table 1 List of working electrodes

Name	R (mm)	A_∞ (mm^2)	E_1	λ_1 (μm)	E_2	λ_2 (μm)
C5Pt	0.252	0.200	1.05	5	1.4	0.25
C7Pt	0.502	0.793	1.10	2	1.25	0.30
C9Pt	0.999	3.135	1.10	2	1.30	0.20

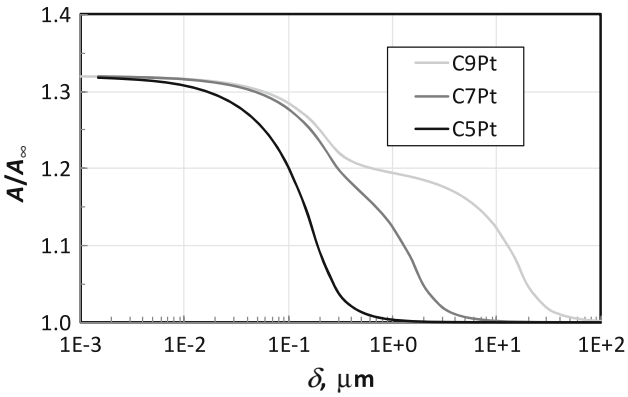

Fig. 7 Plot of the roughness characteristics of the ED probes

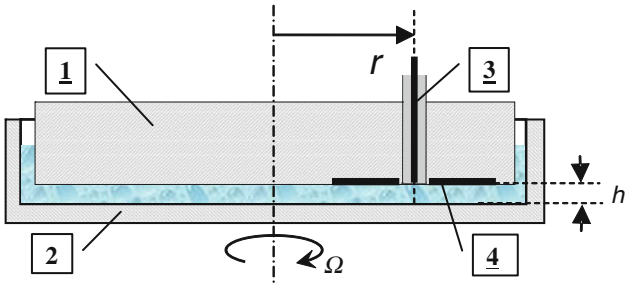

Fig. 8 ED calibrator, $r = 30$ mm, $h = 0.3$ mm. 1, fixed deck; 2, rotating dish; 3, ED probe; 4, large Pt counter electrode

$$\gamma = \Omega r/h. \tag{43}$$

All the tested *electrolyte solutions* contained the potassium ferri-/ferro-cyanide redox couple and potassium sulphate as the supporting electrolyte. Their composition and transport properties at 23 °C are given in Table 2.

The *voltammetric loops* were measured at relatively high shear rate, $\gamma = 100\ \mathrm{s}^{-1}$. Each loop starts at the highest cathodic overvoltage $U = -1200$ mV. After reaching steady cathodic limiting diffusion current, the ramp was driven at a rate of 20 mV s^{-1}. The same process was repeated in the reverse direction: waiting for steady anodic limiting diffusion current and driving the ramp at the same rate. The resulting loops are shown in Fig. 9a–c for a series of the solutions with different concentrations of the depolarizers. A slow absorption process is apparent in the anodic regime. For this reason, the anodic VST curves are neither shown nor treated in this communication.

In all the measurements the ED interface EDIK3 was used [13]. This is a PC-driven bipolar potentiostat with a special current follower covering the ranges from 10 μA to 100 mA. The output current signal (±5 V) was sampled with 12-bit accuracy and frequency 1 kHz (long-time samples) or 100 kHz (short-time samples).

6 Results and discussions

6.1 General approach to data treatment

The experimental VST data were treated with the aim of determining:

- Surface-roughness characteristics $\{A_\infty, \lambda_1, E_1, \lambda_2, E_2\}$ of the ED probes
- Transport properties $\{D_O, D_R, \kappa\}$ of the electrolyte solutions
- Butler–Volmer kinetic data $\{k_{BV}, \beta\}$, which depends on the quality of the working probe surface, and also, to some extent, on the content of the supporting electrolyte, but should be independent of the polarization voltage U.

6.2 Sample fitting: coefficients of diffusion and surface roughness

The cathodic VST curves in motionless electrolyte solutions at large constant voltage step from 0 to −1200 mV were treated to confirm the values of diffusion coefficients obtained from steady and transient convective diffusion [5], and to adjust the roughness characteristics. This fitting procedure results in the calibration data both for ED probes and electrolyte solutions, given in Tables 1 and 2. The agreement of data with the Cottrell asymptote for LDC regime is very good, with dispersion below 2%.

6.3 Sample fitting at medium voltages

Examples of VST curves in a motionless solution at cathodic voltage far below the LDC regime limit but high enough to exceed the limits of the linear theory [3, 8], are shown in Fig. 10a–c. They cover a series of the experiments with a single electrolyte solution (the sample Fi25 Fo25 in Table 2), three Pt probes (Table 1), for three cathodic overvoltage, −200, −400, and −800 mV. Each VST curve is composed from the short-time part (0.01–10 ms, 100 kHz) and the long-time part (1–1000 ms, 1 kHz). The both branches overlap in the interval 1–10 ms. As indicated in Fig. 10a by the horizontal arrows, the starting two points in each branch could have an uncertain time coordinate within one sampling interval, because of the chosen way of triggering.

The theory predictions are shown only for the largest electrode C9Pt using the calibration data from Tables 1 and 2. The corresponding normalized operating parameters $\{\beta, B, P, M, k_L/k_S\}$ are included in the plots.

Table 2 List of electrolyte solutions

Name	c_O (mol m^{-3})	c_R (mol m^{-3})	c_{supp} (mol m^{-3})	D_O (μm^2 ms^{-1})	D_R (μm^2 ms^{-1})	κ (S m^{-1})
Fi25 Fo25 Sulph 230 K	25.0	25.0	230	0.600	0.514	8.7
Fi25 Fo12 Sulph 230 K	25.0	12.5	230	0.603	0.517	7.9
Fi12 Fo25 Sulph 230 K	12.5	25.0	230	0.601	0.515	8.1

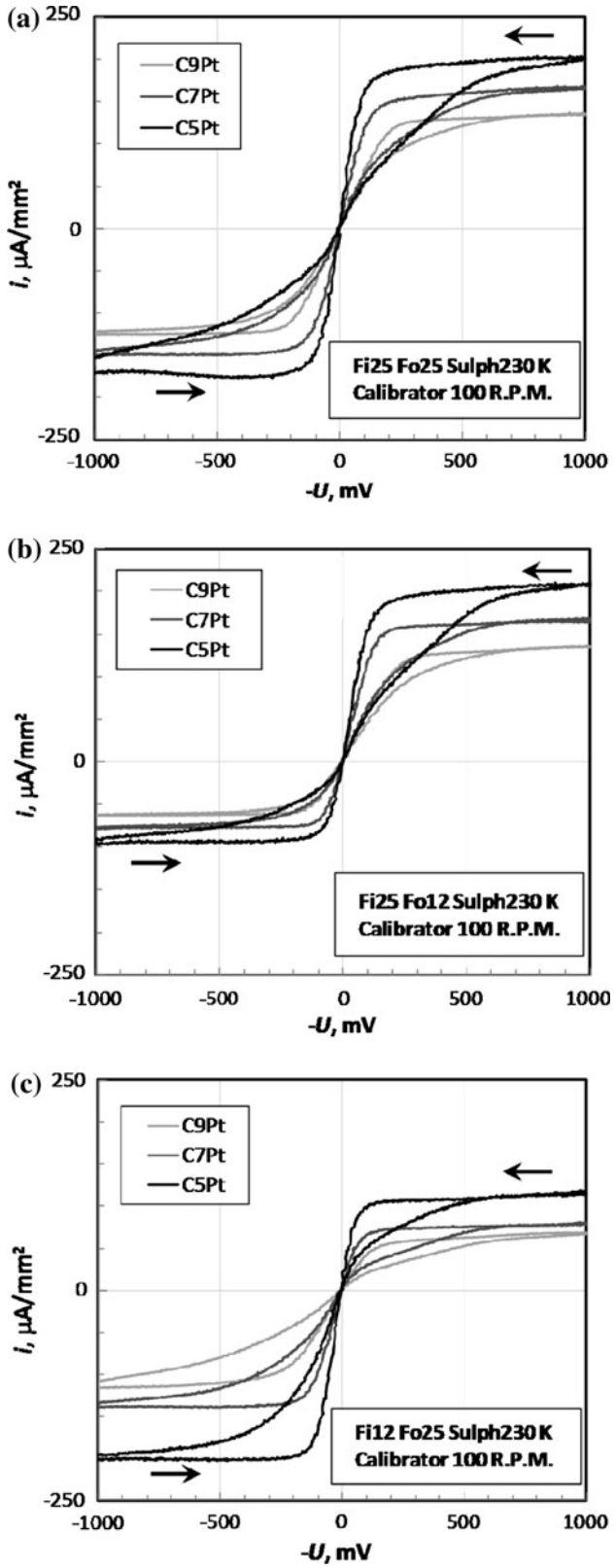

Fig. 9 Voltammetric loops, measured in the ED calibrator at 100 rpm (shear rate 100 s^{-1}) for a series of the ED probes, see Table 1, and various electrolyte solutions, see Table 2. **a** Fi25 Fo25; **b** Fi25 Fo12; **c** Fi12 Fo25. The *arrows* show directions of the individual voltage ramps

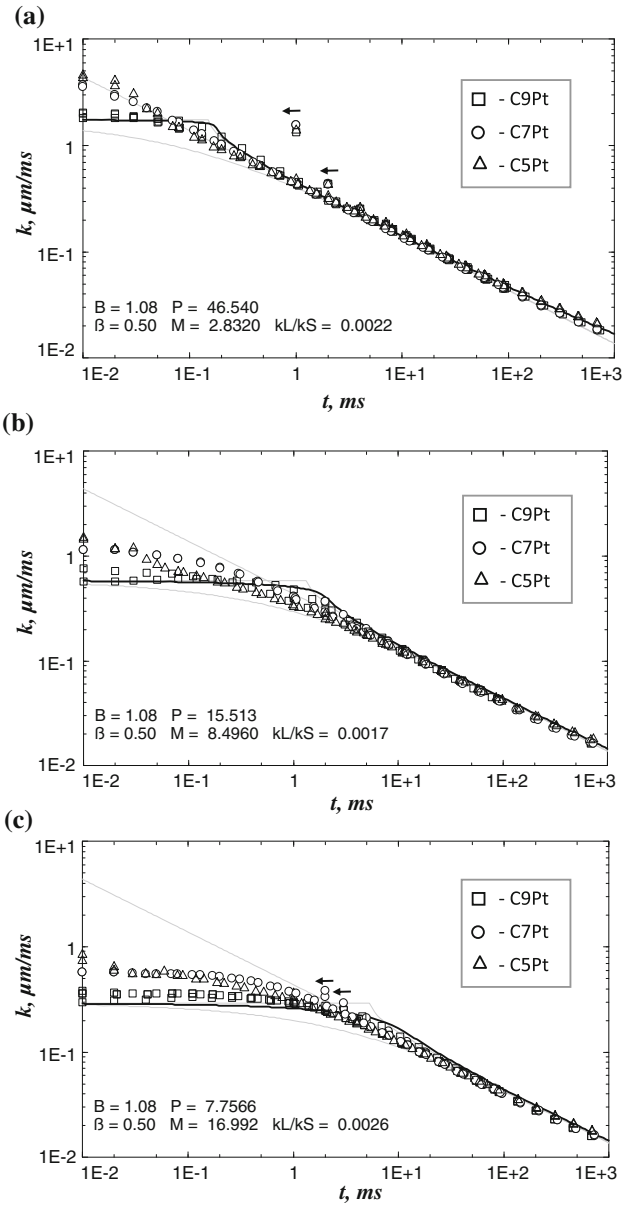

Fig. 10 Voltage-step transient (VST) curves, measured in a still liquid (shear rate 0 s^{-1}) using the beaker ED cell for a series of the ED probes, see Table 1, the electrolyte solutions Fi25 Fo25, see Table 2, at different overvoltage: **a** $U = -800$ mV; **b** $U = -400$ mV; **c** $U = -200$ mV. The *arrows* indicate time uncertainty of a few starting points. The *thick curves* show the fit of the theoretical model on the data for the largest electrode C9Pt

At longer time, say after 5 ms from the start, the VST course, corrected on the edge effect according to Oldham model [10], agrees very well with the Cottrell theory for the reversible electrodes according to Nernst–Petersen [3].

The starting behaviour at shorter time, say below 0.1 ms, is controlled predominantly by the Ohmic losses. At the corresponding resistances about 20–40 Ω, the Faradaic resistance with the rough kinetic estimate $\beta \approx 1/2$,

$k_{BV} \approx 5$ μm ms^{-1} [1, 14] plays a minor role, affecting the starting currents by less than 20%.

It should be noted that the transients do not display the theoretically predicted overshoot in the intermediate range of the VST process, between 0.1 and 1 ms after the start. This discrepancy between 1D theory and experimental data is probably due to neglect of the non-homogeneous field of local overvoltage close to the perimeter of the working electrode.

7 Conclusions

Theory of the early stage of the voltage-step transient (VST) process under effect of Ohmic and Faradaic resistance was enhanced in comparison with [6, 7] by including the galvanometric constraint and by formulating analytical asymptotes. In particular, the extended Cottrell asymptote provides a bridge to the concept of limiting-current regime.

The recent theory of transient convective diffusion [5], which includes 3D effects at higher Peclet number as the edge effects, was combined with the 1D theory [7] to provide a complete semi-empirical model of the full transient process from the start to reaching a steady asymptote. Effect of the electrode surface roughness is included by correcting the mass-transfer coefficients on the area enhancement [12].

The model was used for fitting experimental VST data on a series of electrolyte solutions and circular electrodes in an ED cell with motionless liquid. The data on long-time stage of VST process agree very well with the theory of transient convective diffusion [5], and are used for the calibrations.

The data on the early stage of the VST indicate fairly good agreement with the theory. The Ohmic resistance is a dominant effect (above 70%) while the effect of Faradaic resistance is rather week (below 30%). However, the overshoot of the Cottrell asymptote at high overvoltage predicted by the 1D theory was not observed in the experimental VST data. It seems that the 1D theory is inadequate in a narrow region about the lag time, $t = t_S$ (i.e. $T = 1$), probably because of another 3D effect—the primary current distribution. Including this 3D effect could further improve the theory of the VST process.

Acknowledgment Support by the Czech Science Foundation (GACR) through the projects 104/08/0428 and 104/09/0972 is acknowledged.

References

1. Vetter KJ (1967) Electrochemical kinetics. Academic Press, New York
2. Newman JS (1973) Electrochemical systems. Prentice Hall, Englewood Cliffs
3. McDonald DD (1977) Transient techniques in electrochemistry. Plenum Press, New York
4. Sobolik V, Tihon J, Wein O, Wichterle K (1998) J Appl Electrochem 28:329
5. Wein O, Tovchigrechko VV, Sobolik V (2006) Int J Heat Mass Transfer 49:4596
6. Wein O (1991) J Appl Electrochem 21:1091
7. Wein O (1993) Transient process in a redox system started by a large voltage step. Elektrokhimiya 29:8; in Russian
8. Vielstich W, Delahay P (1957) J Am Chem Soc 79:874
9. Oldham KB, Spannier J (1974) Fractional calculus. Academic Press, New York
10. Oldham KB (1981) J Electroanal Chem 122:1
11. Aoki A, Osteryoung J (1984) J Electroanal Chem 160:335
12. Wein O, Assaf FH (1987) Collect Czech Chem Commun 52:848
13. Wein O (2010) Proceedings of Int. Congr. CHISA 2010
14. Barz F, Bernstein C, Vielstich W (1984) Adv Electrochem Electrochem Eng 13:261